Int. J. Electrochem. Sci., 12 **(2017)** 7869 – 7876, doi: 10.20964/2017.08.70

International Journal of
ELECTROCHEMICAL
SCIENCE
www.electrochemsci.org

Short Communication

Nitrogen-doped Carbon with Hierarchical Porous Structure for Electrocatalysis of Oxygen Reduction Reaction

Xianguo Ma[1], *Shizhong Feng*[2], *Shan Ji*[1,*]

[1] School of Chemical Engineering, Guizhou Institute of Technology, Guiyang, 550003, China,
[2] Gansu petrochina Kunlun Gas Co., Ltd, Lanzhou, 730078, China
[*]E-mail: jissshan@126.com

Received: 12 April 2017 / *Accepted:* 12 June 2017 / *Published:* 12 July 2017

With fuel cells gaining recognition as promising devices for directly converting the chemical energy to electricity, to develop low-cost catalysts for electrocatalysis of oxygen reduction reaction (ORR) has become an active topic in this field. Hierarchical porous carbon materials (HPC) doped with heteroatoms, for instance N, S and Fe, are promising materials for using as catalysts for the ORR due to their low cost, high stability and high efficiency. In this work, we report a low-cost, facile and scalable method to produce nitrogen-doped hierarchical porous carbon material (N-HPC) by pyrolysis of corncobs. The activated N-HPC catalysts exhibit high activity for ORR compared to that of the state-of-the-art commercial Pt/C catalysts.

Keywords: N-doped carbon, Oxygen Reduction Reaction, Electrocatalysis, Biomass.

1. INTRODUCTION

Proton exchange membrane fuel cells hold great promise to directly convert the chemical energy stored in methanol, ethanol and hydrogen into electricity via environmentally friendly electrochemical processes [1-3]. Currently, Pt and Pt-based nanoparticles deposited on carbon supports are widely used as catalysts for fuel oxidation reaction and oxygen reduction reaction (ORR) in fuel cells. Compared to fuel oxidation reaction, electrocatalysis of ORR is the rate determining step of the overall performance of fuel cells due to the sluggish oxygen oxidation reaction [4-6]. Although Pt and Pt-based nanoparticles are considered the most effective electrocatalysts for ORR, they suffer from drawbacks of prohibitive cost, cross-over effect, pure durability and scarcity in supply, which hinder the practical applications of fuel cells [7]. In this regard, precious-metal-free electrocatalysts, such as

carbon and transition metal oxides, have been investigated as alternatives to the current state-of-the-art Pt/C used in fuel cells [8-10].

Among these precious-metal-free catalysts, heteroatom-embedded carbons, such as N(S, P, Fe)-doped carbon, carbon nanotube (CNT) and hierarchical porous carbon (HPC), have been considered as promising alternatives to Pt-based catalyst because of their low cost, good electrical conductivity, high catalytic activity and durability for the ORR [11-13]. In particular, N-doped hierarchical porous carbon stand out due to their considerably high ORR activity, outstanding durability, high methanol/CO tolerance and unique structure. Wang attributed the high electrochemical performance of N-doped carbon to the improved interaction between carbon and N, resulting in an enhanced electron-donor property of the carbon [14].

Many research groups also reported that introducing transition metal elements, such as Fe, Mn and Co, into carbon materials could also enhance the ORR activity in the heteroatom-doped carbon catalyst [14-16]. In the transition metal and nitrogen co-doped carbon materials, the transition metal atoms bonded with the N atoms provide more active sites for the ORR. Although it is difficult to determine the active ORR catalytic sites in deteroatom-doped carbon electrocatalysts, it is found that the ORR activity of those electrocatalysts strongly rely on the precursors of nitrogen and transition-metal, the synthesis conditions and the carbon support morphology [17]. Usually, the N-doped carbon materials can be produced via post-treating carbon materials with N containing materials or directly doping nitrogen atom into carbon during pyrolysis procedure. However, complex processes, expensive equipment or tedious post-treatments are indispensable in the preparation of these N-doped carbons [18-20]. To develop a facile and low-cost method to produce N-HPC with high ORR activity and durability are highly desirable [7, 21].

Corncob as a waste of corn production contain a considerable amount of amino/fibers and small amount minerals, which could serve as the C, N and metal resources for producing heteroatom-doped carbon materials. Based on the recent report from United States Department of Agriculture, global corn production for 2013-14 reached 989.2 million metric tons [22]. Assuming that all current corncobs are collected, 41.1–54.7 million metric tons of corncobs are annually available. If a method can be developed to produce N-HPC from corncob, the waste could be transformed into more value-added products. In the present work, we developed a low-cost method to produce N-HPC with high surface area and hierarchical porous structure from corncobs. It is revealed that the as-prepared N-HPC exhibits a high ORR activity, making it a promising low-cost ORR catalyst for using in fuel cells.

2. EXPERIMENTAL

2.1. Catalysis synthesis

The N-HPC was prepared by direct pyrolysis of corncobs. The detailed procedure of preparing N-HPC from corncobs is as follows: corncobs were first cut into small pieces, and then washed with ultrapure water and dried in a vacuum oven for overnight. The dried starting material was put in a quartz tube furnace, and carbonized at 800 °C for 3 hours in N_2 atmosphere. Subsequently, the sample

was cooled to room temperature, and carbonized sample was ball-milled in a stainless steel jar for 5 hours, and then immersed in 2 mol L^{-1} HNO_3 and 0.5 mol L^{-1} ferric chloride ($FeCl_3$) for 12 hours to remove the impurities. After that, the sample was washed with pure water and then dried in a vacuum oven at 60 °C. The dried sample was heated to 800 °C and kept at this temperature for 3 hours under N_2 atmosphere again. The obtained product was immersed in 2 mol L^{-1} HNO_3 solution for 24 hours to remove unstable Fe species. After that, the sample was rinsed by ultrapure water until pH of the filtrate was 7, and then dried at 60 °C for 12 hours. The final product was labeled as N-HPC.

2.2. Characterizations

X-ray diffraction (XRD) patterns were recorded on a Shimadzu XD-3A (Japan), using filtered Cu-Kα radiation operated at 40 kV and 30 mA. Raman spectroscopy was carried out on a Ft-Raman spectroscopy (RFS 100, BRUKER) with Nd: YAG laser wavelength of 1064 nm. Scanning electronic microscope (SEM) was performed using a JSMF–6701F (JEOL Co., Japan) operated at 5 kV. The specific surface area was measured on a Quantachrome Autosorb-1 volumertic analyzer, using nitrogen adsorption and the Brunauer-Emmett-Teller (BET) method, and the pore size distribution was calculated from the isotherms using the BJH (Barett-Joyner-Halenda) procedure. X-ray photoelectron spectra (XPS) were acquired with a VG Escalab210 spectrometer fitted with Mg 300 W X-ray source. Accurate binding energies were determined by referencing to the C 1s peak at 285.0 eV.

Electrochemical measurements were carried out using an electrochemical workstation (CHI650). For comparison, the commercial Pt/C (E-TEK Corp.) catalysts and XC-72 were used in the electrocatalytic testing processes. A common three-electrode electrochemical cell was used for the measurements. The counter and reference electrodes were a platinum wire and an Ag/AgCl (saturated KCl solution) electrode respectively. Rotating disk electrode (RDE) was used as the working electrode, which was prepared as follows: 5 mg of catalyst was dispersed ultrasonically in 1 mL Nafion/ethanol (0.25% Nafion) and a measured amount of the dispersion was transferred onto the glassy carbon disk (5 mm in diameter) using a pipette and then dried in the air. The ORR activity of the N-HPC samples evaluated on rotating disc electrode (RDE) by linear sweep voltammograms (LSV) in 0.1 mol L^{-1} KOH solution saturated with O_2.

3. RESULTS AND DISCUSSION

The morphology of the obtained N-HPC was first investigated by SEM. Figure 1a shows that irregular particles of N-HPC are formed and the particle distribution is in the range of about 50 ~ 1000 nm. Figure 1b shows the crystal structure of N-HPC which was determined by XRD. It is found that two peaks at ca. 24.8° and 44.5° are observed in the XRD pattern of N-HPC, which can be attributed to the (002) and (101) planes of the graphitic structure [14, 23-26]. There aren't any peaks related to Fe species, suggesting the crystalline Fe species can be completely removed from its surface by the acid treatment.

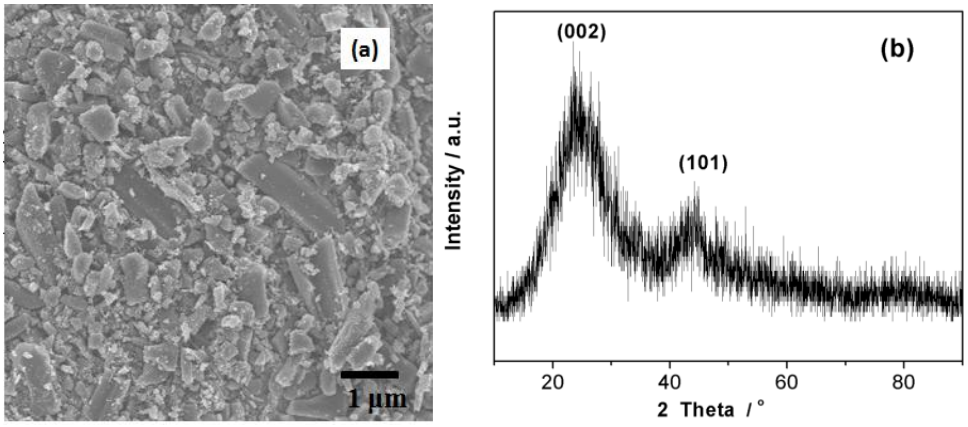

Figure 1. SEM image (a) and XRD pattern (b) of N-HPC.

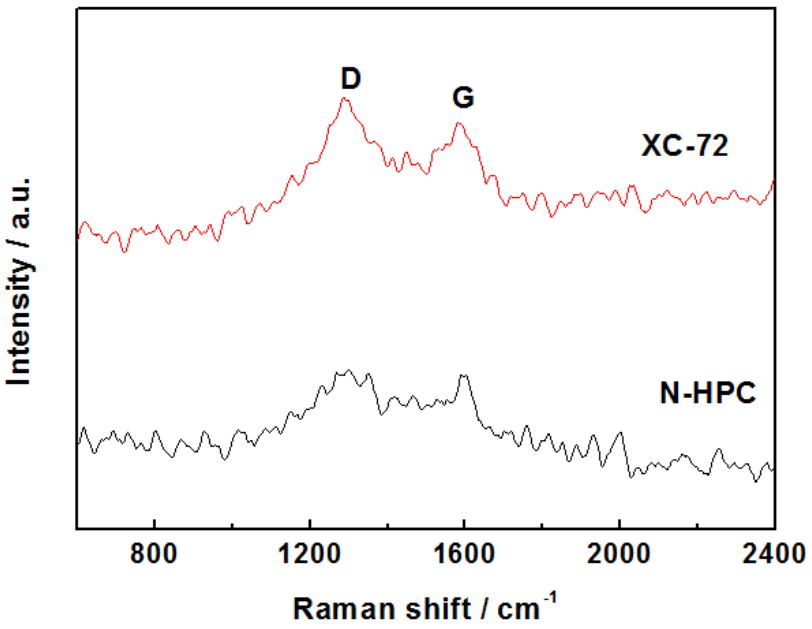

Figure 2. Raman spectra of N-HPC and XC-72

Figure 2 shows Raman spectra of N-HPC and commercial carbon (XC-72). Raman spectra of the two samples exhibits that there are two peaks at ~1300 cm^{-1} and ~1600 cm^{-1}, that correspond to the D band and G band respectively. The Raman D-band is originated from structural defects and partially disordered structures caused by lattice defect, distortion and G-band related to the degree of graphitization of carbon materials [19, 20]. The intensity ratio of I_D/I_G is directly linked to the crystallinity of carbon, namely lower I_D/I_G ratio represents higher crystallinity. As shown in Figure 2, the I_D/I_G of N-HPC is the lower than XC-72, suggesting that the crystallinity of N-HPC is higher than that of XC-72.

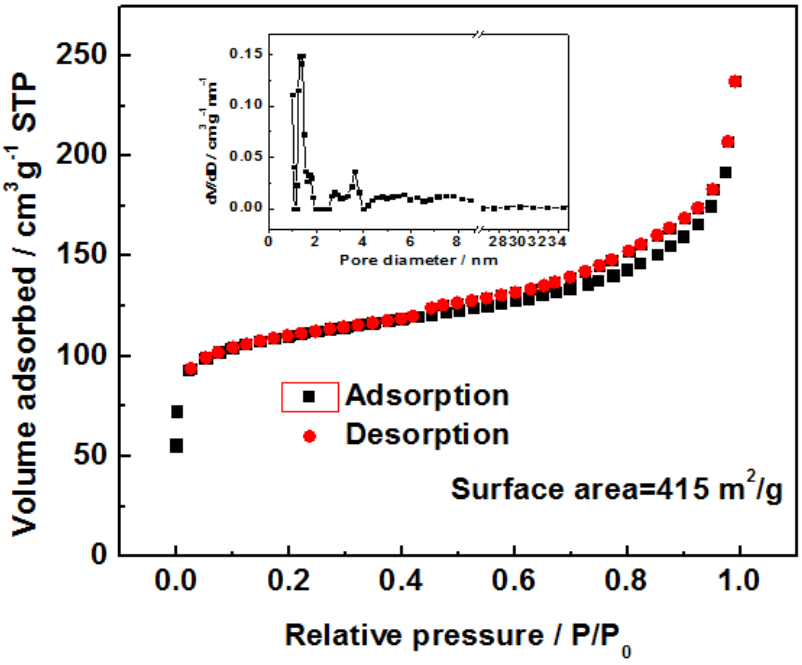

Figure 3. N_2 adsorption-desorption isotherm of N-HPC; Insets: the corresponding pore size distribution.

N_2 adsorption-desorption isotherms of N-HPC and the corresponding specific surface areas and pore sizes are present in Figure 3. The isotherm of N-HPC is a mixed type of the IUPAC classification, namely type I at relative low and intermediated pressure, and type IV at relative high pressure. In the beginning part of isotherm, it is of type I with clearly uptakes which is characteristic of micro-porous materials. Inset of the Figure 3 shows that the diameters of the micro-pores for N-HPC is centered at ~1.50 nm. There isn't clearly plateau at the knee of isotherm, but a clear hysteresis slope is present in the range of intermediate and high relative pressure, implying large micro-pores and meso-pores existed in N-HPC. The BET surface area of N-HPC is ~ 415 m^2 g^{-1}. High surface area is usually associated with high catalytic activity, since more active sites will be available for reactants on the surface.

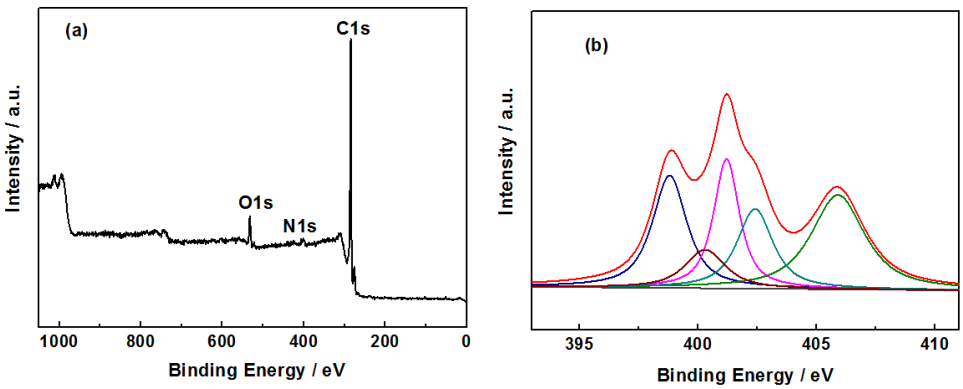

Figure 4. XPS survey spectrum (a) and high resolution XPS spectrum at N1s region (b) of N-HPC.

Figure 4 shows the surface composition (within a depth of 0.1-10 nm) [27] and chemical state of elements of N-HPC investigated by XPS analysis. XPS survey spectra of N-HPC show that there are signals of C 1s, N 1s and O 1s, which confirm the presence of C, O and N elements in N-HPC, while iron signal was absent. After the acid-treatment, unstable iron species were removed, which significantly reduce the amount of iron on the surface. After deconvoluting the high resolution N 1s spectrum, five chemical states of N atoms are found on the surface of N-HPC. The N 1s spectrum of N-HPC (Figure 4b) fitted into five component peaks, which are ascribed to pyridinic-N (BE ~ 398.8 eV), pyrrolic-N (BE ~ 400.3 eV), graphitic-N (BE ~ 401.2 eV), the chemisorbed nitrogen oxide species (BE ~ 402.4 eV), and ammonia (BE ~ 405.9 eV) [28]. Pyridinic-N, which can provide one *p*-electron to the aromatic *p* system, is the N atom linked with two carbon atoms at the brim of graphene plane; the N atom bonded to two C atoms and one H atom forms pyrrolic-like N, which can provide two p-electrons; graphitic-N refers to the N atom bonded to three C atoms and incorporated into the graphene layer. The result of the N 1s spectrum shows that most of N atoms in N-HPC were incorporated into the graphite layers and formed various types of N groups, which play a significant role in improving the electrocatalytic reactions.

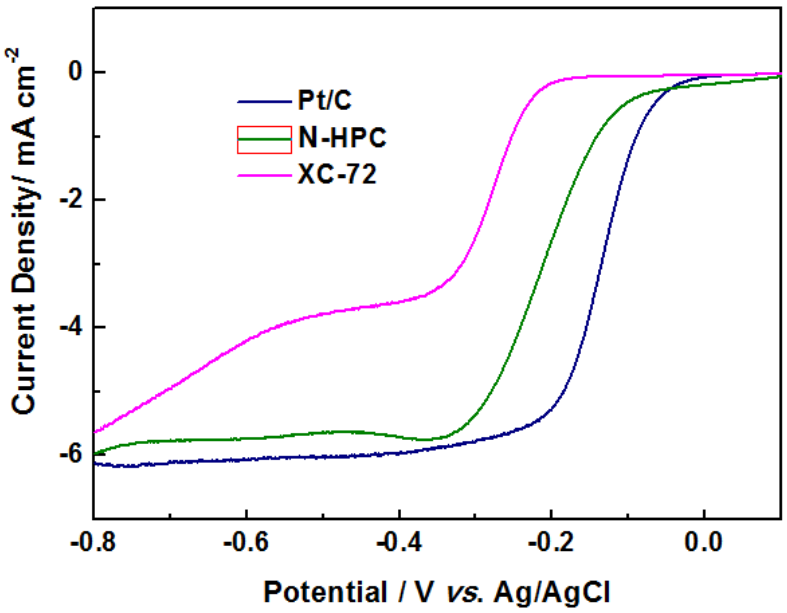

Figure 5. Linear sweep voltammograms of N-HPC, XC-72 and Pt/C for ORR in 0.1 mol L^{-1} KOH aqueous solution at a scan rate of 5 mV s^{-1} and rotation rate of 1600 rpm.

Figure 5 shows the ORR activity of the N-HPC samples evaluated in 0.1 mol L^{-1} KOH solution saturated with O_2 on RDE by linear sweep voltammograms (LSV). For comparison, the ORR polarization curves of commercial Pt/C (10 wt.%) and Vulcan carbon (XC-72) are also present in Figure 5. XC-72 shows very low ORR activity in the KOH aqueous. LSVs of XC-72 shows reducing current started at ~ - 0.3 V without current plateau, which means that the ORR process was mainly a two-electron reduction of O_2 to OOH^-. For N-HPC, the LSVs show a drop at ~0.05 V and rapidly

reached saturation current, which suggest ORR occurred on this samples is a diffusion-controlled process via an efficient $4e^-$ dominated pathway. Figure 5 clearly shows that half-wave potential of N-HPC is only 100 mV more negative than that of XC-72, and the onset potential of N-HPC is slightly lower than that of Pt/C and XC-72, indicating N-HPC is more active than XC-72 and almost comparable to Pt/C in alkaline electrolyte. It also found that the ORR onset potential of N-HPC is lower than many results reported in the literate on the N-doped carbon materials derived from biomass [29, 30], but lower than these N-doped carbon materials with much higher surface areas [23, 31]. The ORR results show this N-HPC is promising N-doped carbon material for catalyzing oxygen reduction reaction in alkaline electrolyte. Although the activity of N-HPC is still not as high as commercial Pt/C, the low-cost, scalable production and abundance in supply make it a promising ORR catalyst as alternative to Pt/C used in alkaline fuel cells.

4. CONCLUSIONS

A high surface area and porous carbon material with high ORR activity was successfully produced from corncobs via a facile and low-cost method. The BET surface area of N-HPC is 415 $m^2 g^{-1}$. XPS results show that most of the N species on N-HPC were in the form of pyridine-N and quaternary-N, which are considered to be the active species for the ORR. Compared with the Pt/C (10 wt.%), the N-HPC exhibits a comparable ORR electrocatalytic activities in KOH solution. Therefore, N-HPC is a promising alternative material to commercial Pt/C for ORR in alkaline solution due to its high activity, low cost and easy synthesis.

ACKNOWLEDGEMENTS
The authors would like to thank the National Natural Science Foundation of China (No. 51603049) and Natural Science Foundation of Guizhou Province (No. qian ke he J zi [2015]2059) for financially supporting this work.

References

1. Y. Ma, H. Li, H. Wang, S. Ji, V. Linkov, R. Wang, *Journal of Power Sources,* 259 (2014) 87-91.
2. I. Katsounaros, S. Cherevko, A.R. Zeradjanin, K.J.J. Mayrhofer, *Angewandte Chemie International Edition,* 53 (2014) 102-121.
3. M. Rahimi-Esbo, A. Ramiar, A.A. Ranjbar, E. Alizadeh, *International Journal of Hydrogen Energy,* 42 (2017) 11673-11688.
4. Y. Ma, R. Wang, H. Wang, S. Ji, *Int. J. Electrochem. Sci,* 8 (2013) 6085-6093.
5. P. Bosch-Jimenez, S. Martinez-Crespiera, D. Amantia, M. Della Pirriera, I. Forns, R. Shechter, E. Borràs, *Electrochimica Acta,* 228 (2017) 380-388.
6. K.-H. Wu, D.-W. Wang, X. Zong, B. Zhang, Y. Liu, I.R. Gentle, D.-S. Su, *Journal of Materials Chemistry A,* 5 (2017) 3239-3248.
7. R. Wang, H. Song, H. Li, H. Wang, X. Mao, S. Ji, *Journal of Power Sources,* 278 (2015) 213-217.
8. Y. Ma, R. Wang, H. Wang, J. Key, S. Ji, *Journal of Power Sources,* 280 (2015) 526-532.
9. K. Niu, B. Yang, J. Cui, J. Jin, X. Fu, Q. Zhao, J. Zhang, *Journal of Power Sources,* 243 (2013) 65-

71.
10. G. Liu, X. Li, P. Ganesan, B.N. Popov, *Electrochimica Acta*, 55 (2010) 2853-2858.
11. H. Wang, W. Wang, J. Key, S. Ji, Y. Ma, L. Khotseng, W. Lv, R. Wang, *J Solid State Electrochem*, 19 (2015) 1181-1186.
12. H. Yang, H. Li, H. Wang, R. Wang, *Fuel Cells*, 15 (2015) 214-220.
13. M. Watanabe, D.A. Tryk, M. Wakisaka, H. Yano, H. Uchida, *Electrochimica Acta*, 84 (2012) 187-201.
14. H. Yang, H. Li, H. Wang, S. Ji, J. Key, R. Wang, *Journal of The Electrochemical Society*, 161 (2014) F795-F802.
15. Z.-Y. Wu, P. Chen, Q.-S. Wu, L.-F. Yang, Z. Pan, Q. Wang, *Nano Energy*, 8 (2014) 118-125.
16. J. Masa, W. Xia, I. Sinev, A. Zhao, Z. Sun, S. Grützke, P. Weide, M. Muhler, W. Schuhmann, *Angewandte Chemie International Edition*, 53 (2014) 8508-8512.
17. X. Liu, H. Zhu, X. Yang, *Journal of Power Sources*, 262 (2014) 414-420.
18. F. Liu, H. Peng, C. You, Z. Fu, P. Huang, H. Song, S. Liao, *Electrochimica Acta*, 138 (2014) 353-359.
19. T. Zhou, H. Wang, J. Key, S. Ji, V. Linkov, R. Wang, *RSC Advances*, 3 (2013) 16949.
20. K. Wang, H. Wang, S. Ji, H. Feng, V. Linkov, R. Wang, *RSC Advances*, 3 (2013) 12039-12042.
21. Z. Zhang, H. Li, Y. Yang, J. Key, S. Ji, Y. Ma, H. Wang, R. Wang, *RSC Advances*, 5 (2015) 27112-27119.
22. W.-H. Qu, Y.-Y. Xu, A.-H. Lu, X.-Q. Zhang, W.-C. Li, *Bioresource Technology*, 189 (2015) 285-291.
23. R. Wang, H. Wang, T. Zhou, J. Key, Y. Ma, Z. Zhang, Q. Wang, S. Ji, *Journal of Power Sources*, 274 (2015) 741-747.
24. R. Chetty, S. Kundu, W. Xia, M. Bron, W. Schuhmann, V. Chirila, W. Brandl, T. Reinecke, M. Muhler, *Electrochimica Acta*, 54 (2009) 4208-4215.
25. R. Wang, T. Zhou, H. Wang, H. Feng, S. Ji, *Journal of Power Sources*, 269 (2014) 54-60.
26. L. Chen, X. Cui, Y. Wang, M. Wang, F. Cui, C. Wei, W. Huang, Z. Hua, L. Zhang, J. Shi, *Chemistry – An Asian Journal*, 9 (2014) 2915-2920.
27. H. Niu, Y. Wang, X. Zhang, Z. Meng, Y. Cai, *ACS Applied Materials & Interfaces*, 4 (2012) 286-295.
28. Y. Ma, H. Wang, H. Feng, S. Ji, X. Mao, R. Wang, *Electrochimica Acta*, 142 (2014) 317-323.
29. Y. Ma, J. Zhao, L. Zhang, Y. Zhao, Q. Fan, X.a. Li, Z. Hu, W. Huang, *Carbon*, 49 (2011) 5292-5297.
30. J. Lu, X. Bo, H. Wang, L. Guo, *Electrochimica Acta*, 108 (2013) 10-16.
31. S. Li, R. Xu, H. Wang, D.J.L. Brett, S. Ji, B.G. Pollet, R. Wang, *J Solid State Electrochem*, (2017) 1-8.